Food Chemistry: X 13 (2022) 100250

Contents lists available at ScienceDirect

Food Chemistry: X

journal homepage: www.sciencedirect.com/journal/food-chemistry-x

Comparative transcriptomics discloses the regulatory impact of carbon/nitrogen fermentation on the biosynthesis of *Monascus kaoliang* pigments

Aijun Tong [a], Jinqiang Lu [a], Zirui Huang [a], Qizhen Huang [a], Yuyu Zhang [b,c,*], Mohamed A. Farag [d], Bin Liu [a,*], Chao Zhao [a,b,*]

[a] College of Food Science, Fujian Agriculture and Forestry University, Fuzhou 350002, China
[b] Key Laboratory of Brewing Molecular Engineering of China Light Industry, Beijing Technology and Business University (BTBU), Beijing 100048, China
[c] Beijing Key Laboratory of Flavor Chemistry, Beijing Technology and Business University (BTBU), Beijing 100048, China
[d] Department of Pharmacognosy, Faculty of Pharmacy, Cairo University, Cairo 11562, Egypt

ARTICLE INFO

Keywords:
Monascus pigments
Carbon metabolism
Nitrogen metabolism
Transcriptomic

ABSTRACT

Carbon and nitrogen play a fundamental role in the production of *Monascus* pigments. However, their effects on pigment biosynthesis remain undetermined. In this study, we found that *Monascus kaoliang* produces pigments via liquid fermentation using glycerol and peptone as suitable carbon and nitrogen sources, respectively. Comparative transcriptomic profiling was performed using RNA sequencing. It indicated that the differentially expressed genes (DEGs) of carbon were enriched using amino acids and carbohydrates via the transport and metabolism pathways, respectively. DEGs of nitrogen were enriched only using general functional prediction pathways. These data provide a comprehensive interpretation of the linkage between primary and secondary metabolisms in *M. kaoliang*. Moreover, they provide insights into the effects of various substances involved in secondary metabolism.

1. Introduction

Fermentation products from *Monascus* spp., known as red rice, hong qu, or dan qu in ancient times, is widely used in Fujian, Zhejiang, Jiangxi, Guangdong, and Taiwan (Park et al., 2016). People have always favored red rice as a traditional Chinese medicine that can also be used as food. *Monascus* spp. can generate plenty of secondary metabolites, including pigments, monacolin K, γ-aminobutyric acid, and dimerumic acid (Aniya et al., 2000; Chen et al., 2015; Diana et al., 2014). *Monascus* pigments (MPs) are important secondary metabolites that can substitute some synthetic pigments in the food industry (Shi et al., 2015). The European Union and the United States recognize MPs as food coloring agents. They can also be used as substitutes for nitrates and nitrites in seasoning and preserving red meat (Mapari et al., 2010; Agboyiboret al., 2018). MPs can effectively lower blood pressure, reduce plasma cholesterol levels, prevent obesity, and improve anti-inflammatory activity. Moreover, they can be used to prevent cancer, reduce blood sugar levels, and possess anti-inflammatory and anti-tumor properties (Yasukawa et al., 1996; Nam et al., 2014; Zhang et al., 2021).

The bioynthesis of MPs depends on many factors, such as *Monascus* spp. strain, carbon source, nitrogen source, nitrogen to carbon ratio, pH value, and other nutritional and environmental factors (Said et al., 2014; Chen et al., 2017; Patrovsky et al., 2019; Yang et al., 2021). Many have reported that regulating the culture medium composition and conditions improves the yield of health-related metabolite in *Monascus* spp., such as yellow pigments. It also reduces the production of citrinin, a toxic substance (Hajjajet al., 2015; Chenet al., 2017). Nature of the carbon source and difficulties in utilizing it directly affects the metabolic rate of *Monascus* spp. Subsequently, affecting substance synthesis and degradation, and impairing the production of MPs (Embabyet al., 2018). Glycerol promotes MP production and more substrates might be generated from glycolysis and carbon metabolism for the biosynthesis of MPs (Zhao et al., 2019; Shi et al., 2020). Pigment production was also found to be dramatically elevated with glycerol used as the sole carbon source compared with other carbon sources (Huang et al., 2018).

Using nitrogen sources also affects the composition of the MPs extensively. NH_4Cl and $(NH_4)_2SO_4$ are favorable for the synthesis of orange or yellow pigments. When $(NH_4)_2SO_4$ is used as the nitrogen source, the intracellular pigment is mainly red; however, a small amount of yellow is also present. When peptone is used as the nitrogen source,

* Corresponding authors at: No. 15 Shangxiadian Rd., Fuzhou 350002, China.
E-mail addresses: zhangyuyu@btbu.edu.cn (Y. Zhang), liubin618@hotmail.com (B. Liu), zhchao@live.cn (C. Zhao).

https://doi.org/10.1016/j.fochx.2022.100250
Received 26 September 2021; Received in revised form 20 December 2021; Accepted 4 February 2022
Available online 7 February 2022

several red pigment derivatives dominate the cytochrome. Neither peptone nor $(NH_4)_2SO_4$ facilitates the generation of intracellular orange pigment. However, a higher yield of extracellular orange pigment has been observed, especially when using peptone. Nitrate and organic nitrogen sources promote the formation of the red pigment (Lin and Demain, 1995; Shi et al., 2015; Zhou et al., 2020). Our previous study has shown that NH_4Cl or NH_4NO_3can promote the precursor synthesis ofMPs (Hong et al.,2020). Growth and secondary metabolism are differently impacted by various cofactors (Liu et al., 2020). Although many investigations have assessed the impacts of different carbon and nitrogen sources on the production of MPs, few have elucidated the mechanisms involved in regulating their production using these sources via *Monascus* spp. fermentation and transcriptomics.

MPs are ketones produced by *Monascus* spp. fermentation. The key enzymes in the biosynthetic pathway of MPs include the following: polyketide synthase, G protein signaling pathway, polypeptide synthase, lipotin synthase, transcriptional activator, acyltransferase, oxidoreductase, and hydroxylase (Li et al., 2010; Klinsupa et al., 2016). In this study, the liquid fermentation conditions were optimized to obtain the most suitable carbon and nitrogen sources, and *M. Kaoliang* (T3) was regulated using them. Transcriptome analysis was conducted to study the characteristics of different metabolites from various carbon and nitrogen sources.

2. Materials and methods

2.1. Identification of strains and culture conditions

The T3 used in this experiment was isolated from hongqu provided by Nanping County, Fujian Province, China. T3 was cultured at 30℃ for 7 d in potato dextrose agar (PDA) and then stored at 4℃ till further analysis. The isolated and purified strains were inoculated on wort medium 15°BX (WA), agar for extracting powder from Chardonnay yeast (CYA), agar for extracting malt powder (MEA), and glycerol nitrate agar (G25N) media using spot seeding method. The strains were cultured at 25℃ for 7 d. Then, the colony characteristics were observed. All the chemical reagents were supplied by Sinopharm Chemical Reagent Co., Ltd and Guangdong Huankai Microbial Sci. & Tech. Co., Ltd. (Guangzhou, China). The chemical reagents were analytically pure.

Taq DNA polymerase was purchased from Dalian TaKaRa Co., Ltd. Primer, phenol/chloroform/isoamyl alcohol (25:24:1), chloroform/isoamyl alcohol (24:1), 100 bp DNA maker, GoldView nucleic acid dye, and agar sugar were purchased from Sangon Biological Engineering Co., Ltd (Shanghai, China). Gradient PCR instrument was purchased from MJ Company, USA and agarose horizontal plate electrophoresis instrument was purchased from Beijing Liuyi Company. Genomic DNA from *Monascus* hyphae was extracted using two pairs of primers:ITS1/ITS4 and β-tubulin-F/β-tubulin-R. They were used to amplify different regions of ITS-5.8SrDNA. The PCR product obtained was verified using agarose gel electrophoresis. Direct two-way sequencing was done using the sequencer ABI3730. The tested sequences were compared for similarity using the GenBank database with Blast software.

2.2. Fermentation media

The fermentation medium was composed of 8% carbon source (soluble starch, mannitol, α-lactose, fructose, sucrose, or glycerol), 1.5% nitrogen source (yeast powder, $NaNO_3$,$(NH4)_2SO_4$, peptone, monosodium glutamate, or corn steep liquor), 0.25% KH_2PO_4, 0.1% $MgSO_4{\cdot}7H_2O$, and 100 mL distilled water in a 250 mL flask. It was incubated at 30℃ in a rotary shaker at 180 rpm. The prepared medium was sterilized at 121℃ for 20 min. PDA slants and sterile water (30℃, 7 d) were used to prepare spore suspensions,and the concentration was adjusted to 1.0×10^6 colony-forming unit/mL.

2.3. MPs content

The fermentation broth (0.5 mL) was purified using 10 mL of 70% ethanol followed by oscillation in a centrifuge tube, which was allowed to stand for 1 h. Then, it was subjected to filtration. The supernatant was analyzed using a spectrophotometer (UV-2601, Beifen-Ruili, Beijing) against a 70% ethanol solution. The contents of the yellow, orange, and red pigments were determined at wavelengths of 410, 465, and 510 nm, respectively. Their concentrations were calculated using the following formula: color value (U/mL)=$(OD_{410} + OD_{465} + OD_{510})$*dilution ratio (Lv et al., 2012).

2.4. RNA isolation and high-throughput sequencing (HTS)

Transcriptome analysis was done using the mycelium obtained on day 9 of the T3 fermentation with SP (8% soluble starch, 1.5% peptone, 0.25% KH_2PO_4, 0.1% $MgSO_4{\cdot}7H_2O$, and 100 mL distilled water in a 250 mL flask at 30℃ on a rotary shaker at 180 rpm), GP (8% glycerin, 1.5% peptone, 0.25% KH_2PO_4, 0.1% $7H_2O{\cdot}MgSO_4$, and 100 mL distilled water in a 250 mL flask at 30℃ on a rotary shaker at 180 rpm), and GA (8% glycerin, 1.5% $(NH_4)_2SO_4$, 0.25% KH_2PO_4, 0.1% $MgSO_4{\cdot}7H_2O$, and 100 mL distilled water in a 250 mL flask at 30℃ on a rotary shaker at 180 rpm). Total RNA was isolated using the Trizol reagent following. Libraries were constructed and HTS was carried out on an Illumina HiSeq™ 2500 sequencing platform (Illumina™, San Diego, CA, USA) by the Biomarker Biotechnology Corporation (Beijing, China). The purity, concentration, and integrity of RNA samples were determined using Nanodrop Qubit 2.0 and Agilent 2100 to ensure the quality of the samples being used for transcriptome sequencing.

2.5. Sequencing read assembly, mapping, and annotation

The raw data of FASTQ format were processed using in-house Perl scripts. The adapter-containing, ploy-*N*-containing, and low-quality reads were eliminated from the raw data to obtain the clean reads. The contents of Q10, Q20, Q30, and Q40 in the clean data were calculated. All subsequent assays were performed using high-quality clean data.

2.6. De novo assembly and functional annotation

The joint sequences and low-quality reads were eliminated from the raw data through filtration. The clean data were assembled to construct the UniGene library for these species. Subsequently, Trinity was used for sequence assembly. For functional annotation, all UniGene sequences were searched against several databases, including the NCBI non-redundant protein sequences (NR; ftp://ftp.ncbi.nih.gov/blast/db), Swiss-Prot (http://www.uniprot.org/), Gene Ontology (GO; http://www.geneontology.org/), Clusters of Orthologous Groups (COG; http://www.ncbi.nlm.nih.gov/COG/), and Kyoto Encyclopedia of Genes and Genomes (KEGG; http://www.genome.jp/kegg/).

2.7. Gene expression and differential expression analysis

Bowtie was used to compare the obtained reads by sequencing each sample with the UniGene library. According to comparative gene expression results, the expression was assessed after combining with RSEM. The value of fragments per kilobase per million mapped reads was adopted to represent the abundance of expression of the corresponding UniGene. In the differential expression analysis, the Benjamini-Hochberg method was adopted to correct the p-value obtained from the original hypothesis. Eventually, the adjusted *p*-value, namely false discovery rate (FDR), was the key index in identifying differentially expressed genes (DEGs). A volcano plot for visualizing, FDR < 0.01, and fold change (FC) ≥ 2 were selected as the screening criteria to minimize false positives from independent statistical

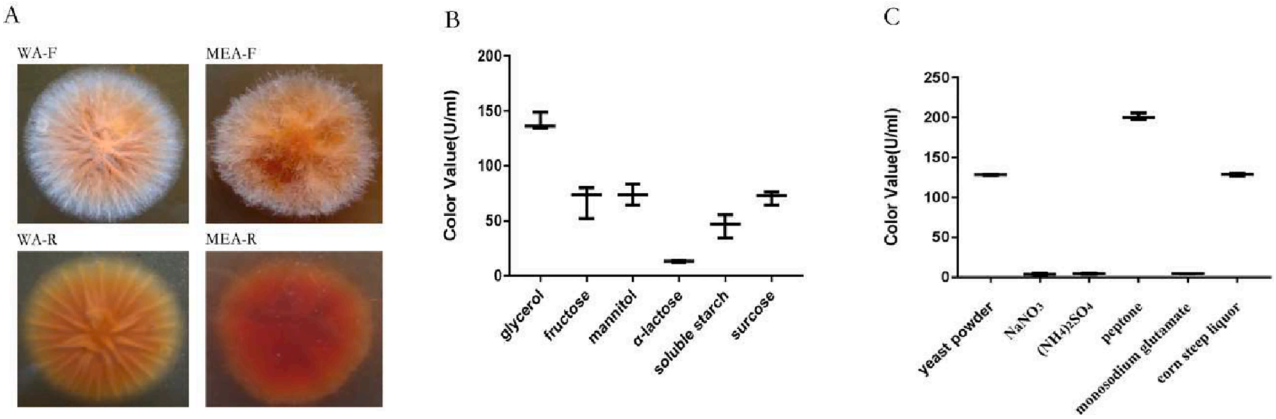

Fig. 1. (***A***) The front and back colony characteristics of *M. kaoliang* T3 growing on Wa/MEA culture medium for 7 d (the chart labeled R on the left bottom represents the back colony). (***B*** and ***C***) the comparison of various carbon/nitrogen sources in pigment production. The error bars indicate the standard deviations of three independent cultures.

Table 1
Identification of the strain T3 through physiological and biochemical test.

Strain	Gelatin hydrolysis	Carbon source utilization					
		Glucose	Maltose	α-Lactose	Fructose	Sucrose	Sorbose
T3	–	++++	++++	++	++	++	+

Note: in the gelatin hydrolysis test,"++" means complete hydrolysis, "+" means mild hydrolysis, and "-" means negative; carbon source utilization: "++++" means grows well, "+++" means good growth, "++" means growth is better, and "+" means growth is average.

Table 2
Sequencing identification of the strain T3.

ITS1/ITS4			β-tubulin-F/β-tubulin-R		
Species	Gene number	Identity (%)	Species	Gene number	Identity (%)
M. kaoliang	AB477252.1	544/545 (99%)	*M. purpureus*	JX221438.1	786/786 (100%)
M. purpureus	AB477247.1	544/545 (99%)	*M. sanguineus*	JX221433.1	764/782 (98%)
M. aurantiacus	DQ978995.1	543/544 (99%)	*M. ruber*	JX221435.1	760/781 (97%)
M. rutilus	DQ978997.1	543/544 (99%)	*M. pilosus*	JX221434.1	760/781 (97%)
M. ruber	AB477256.1	538/541 (99%)	*M. kaoliang*	AB477266.1	602/602 (100%)
Monascus sp.	KC756831.1	544/548 (99%)	*Monascus* sp.	AY498591.1	628/647 (97%)

hypotheses while testing a large number of genes.

3. Results & discussion

3.1. Strain identification and the impacts of carbon/nitrogen sources on the yields of MPs

The wild strain was identified as *M. kaoliang* after observing colony characteristics, physiological and biochemical tests, and molecular biological analysis (Li and Guo, 2003; Li et al., 2009). Partial results of the colony characteristics are shown in Fig. 1A. Since T3 can grow on all four media (WA, MEA, CYA, and G25N) and the colonies are colored (non-white, non-white-green, and non-pink), all of them can be preliminarily excluded. It can beassumed that none of them belongs to *M. eremophilus*, *M. albidus*, *M. pallens*, *M. floridanus*, and *M. pilosus*. The hydrolyzed gelatin test for T3 was negative. Therefore, it could use glucose and maltose. There was no difference in the growth in glucose-containing medium; it could also grow on sucrose, fructose, and sorbose. The above results showed that T3 cannot be *M. purpureus* (Table 1).

In this experiment, two pairs of primers ITS1/ITS4 and β-tubulin-F/β-tubulin-R were used to amplify and sequence different fragments of the ITS1-5.8SrDNA-ITS2 gene and to identify the species of T3, respectively. Furthermore, the amplified ITS1/ITS4 fragments show maximum similarity with *M. kaoliang*, while the amplified β-tubulin-F/β-tubulin-R fragments show maximum similarity with *M. purpureus* (Table 2). Based on the morphological, physiological, and biochemical identification results, it can be concluded that the target strain T3 is *M. kaoliang*.

After liquid fermentation, the pigments produced by *M. kaoliang* were qualitatively and quantitatively determined. Lactose, mannitol, fructose, glycerin, soluble starch, and sucrose were selected as carbon sources (the nitrogen source is peptone during that comparison) to determine their color values. The impacts of various carbon sources on the yield of MPs were studied. The type of carbon source had a significant effect on the yield of pigments. The impacts of 6 different carbon sources on the yields of alcohol-soluble pigments in liquid fermentation can be ranked in descending order as follows: glycerol, mannitol, sucrose, fructose, soluble starch, and lactose. The glycerol-produced pigment had the highest color value of 139.913 U•mL^{-1}, followed by mannitol with a color value of 73.96 U•mL^{-1}. Therefore, glycerol and soluble starch were selected as carbon sources to assess the impacts on the yield of pigments produced by *Monascus* spp. fermentation.

Meanwhile, 6 different nitrogen sources were selected to assess their effects on the yield of MPs. The type of nitrogen source had a great influence on the production of MPs (Fig. 1). According to the pigment production capacity, the color value of alcohol-soluble pigments can be ranked in descending order as follows: peptone, corn milk, yeast powder, ammonium sulfate, sodium glutamate, and sodium nitrate (the carbon source is glycerin during that comparison). Therefore, peptone

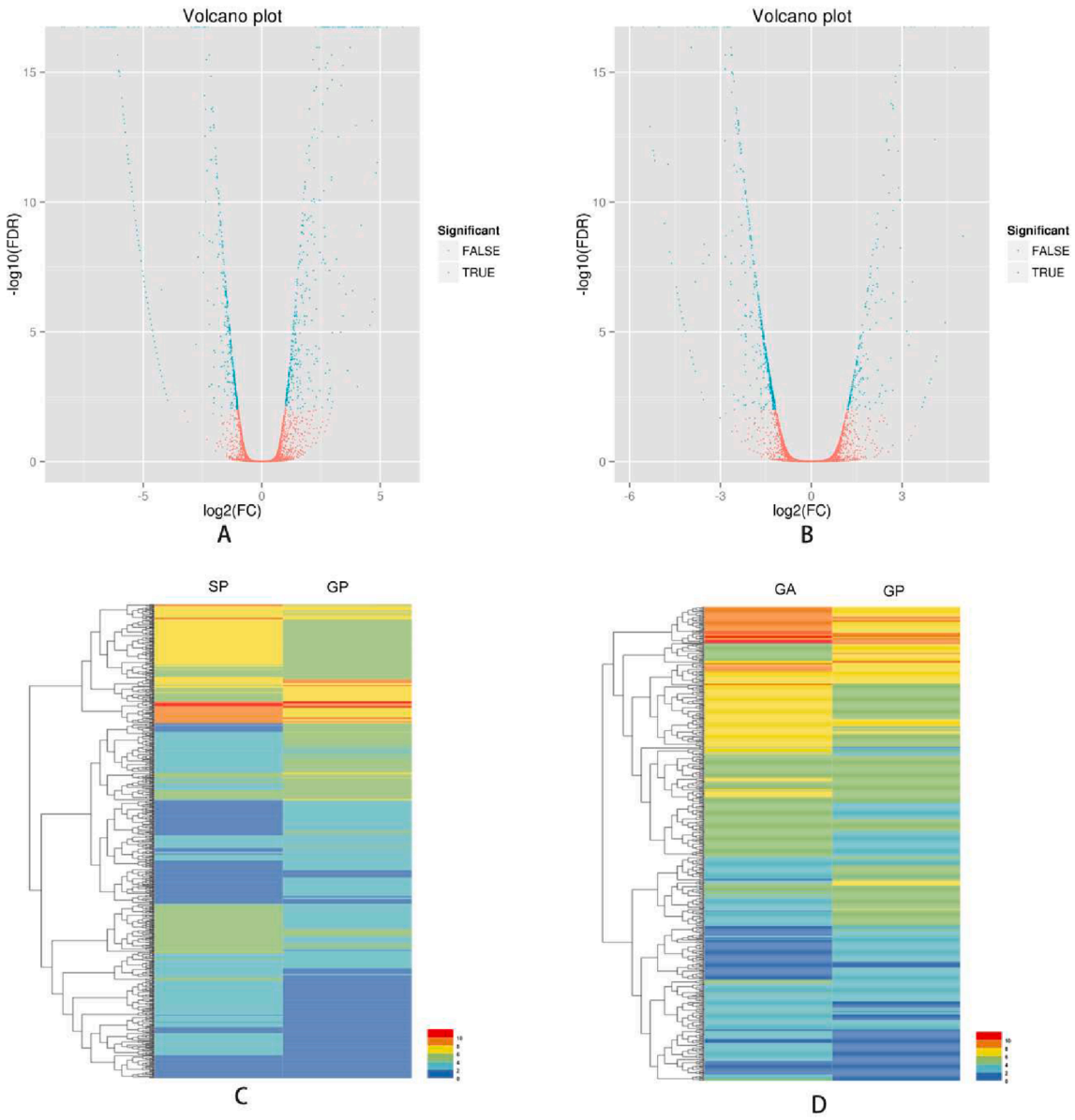

Fig. 2. volcano plot analysis and cluster analysis of DEGs in SP, GP, and GA groups. (***A*** and ***B***) The volcano plot showing the comparison of DEGs in *SP vs GP* and *GA vs GP* groups, respectively. (***C*** and ***D***) The clustering map of DEGs in *SP vs GP* and *GA vs GP* groups, respectively.

showed the strongest effect among all tested nitrogen sources, with a total color value of 201.2 U•mL^{-1}. In contrast, sodium glutamate and sodium nitrate produced the lowest color values and the mycelium grew slowly. Therefore, peptone and $(NH_4)_2SO_4$ were selected as nitrogen sources to assess the effect on the yield of pigments produced by fermenting *Monascus* spp.

The different carbon/nitrogen quality evaluation of sequencing data

To explore the regulatory mechanisms of carbon (*SP vs GP*)/nitrogen (*GA vs GP*) in the biosynthetic pathways of pigments in *M. kaoliang*, an Illumina HTS platform was used to assess the gene transcripts level. For the three samples, the total number of clean data was 12.38 GB, each reaching 4.10 GB, and the quality score of more than 30 reading percentages was about 85%. Therefore, the results of the transcriptome sequencing met the quality requirements of subsequent assembly analysis. All clean data were pooled and assembled using Trinity. A total of 61,933 scripts and 8527 UniGenes were obtained from the assembly, and the N50 of the transcript and UniGene were 8936 and 4696, respectively, indicating high assembly integrity.

3.3. Analysis of DEGs

In this study, 865 and 695 DEGs were identified in the *SP vs GP* and G*A vs GP* groups, respectively. The volcano plots illustrating the distribution of the fold changes and *p*-values were shown in the Fig. 2. The up-regulated and down-regulated DEGs in the "*SP vs GP*" group were 378 and 487, respectively (Fig. 2A). The up-regulated and down-regulated DEGs in the "*GA vs GP*" group were 198 and 461, respectively (Fig. 2B). In the "*GA vs GP*" group, the number of down-regulated genes was higher compared with the up-regulated genes. Hierarchical clustering analysis was conducted on the screened DEGs. The genes with the same or similar expression behaviors were clustered to show the differentially expressed patterns of gene sets under various experimental conditions. The DEG clustering results of various samples are shown (Fig. 2C & 2D). These results indicated that many genes were differentially expressed in the fermentation medium containing various carbon and nitrogen sources.

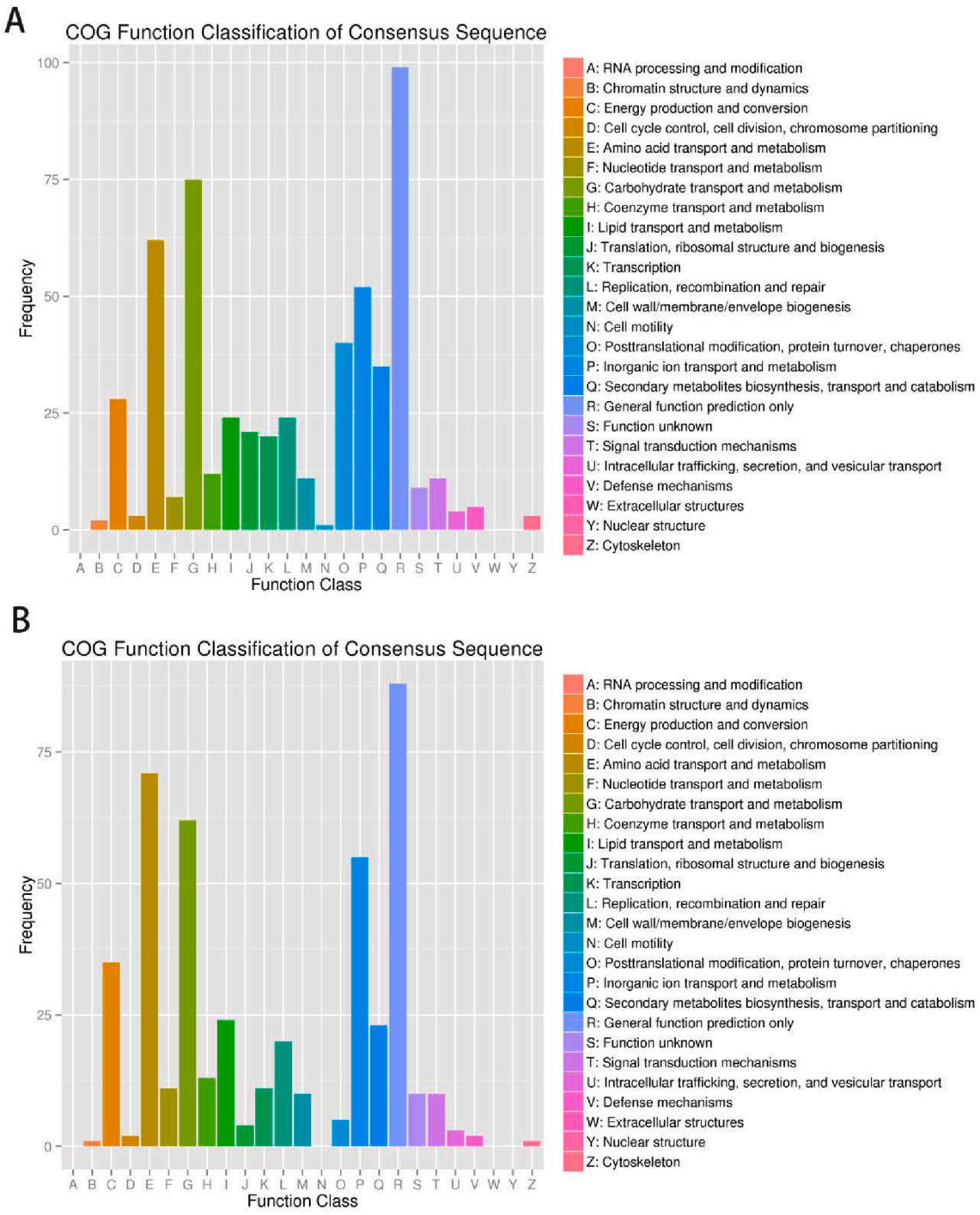

Fig. 3. (***A***and ***B***) COG functional classification of DEGs in the *SP vs GP* and *GA vs GP* groups.

3.4. Functional annotation and enrichment analysis of DEGs

The annotated number of the DEGs based on different functional databases is presented in Table S1. A total of 1372 DEGs were annotated by five commonly used functional databases, including COG, GO, KEGG, Swiss-Prot, and NR (Table S1). Through the COG functional annotation method, the newly generated UniGenes were compared with the COG database to analyze the coding proteins and their evolutionary relationship (Fig. 3A & 3B). The DEGs annotated by COG were assigned into 25 functional categories. "General functional prediction only";"amino acid transport and metabolism"; and "carbohydrate transport and metabolism" were the most frequently annotated functional categories in the "*SP vs GP*" and "*GA vs GP*" groups. Moreover, 35 and 23 DEGs were annotated as "secondary metabolites biosynthesis, transport, and catabolism" in the "*SP vs GP*"and "*GA vs GP*" groups, respectively.

GO enrichment analysis showed that DEGs were categorized into 58 and 56 functional groups in *SP vs GP* and *GA vs GP*, respectively (Fig. 4A & 4B; Table S2). In the cellular component category, "cell", "cell part", "organelle", "membrane", "organelle part macromolecular complex", "membrane part", "extracellular region", and "membrane-enclosed lumen" were the most mapped terms. In the molecular function category, "catalytic activity", "binding transporter activity", and "structural molecule activity" were the most mapped terms. In the biological process category, "metabolic process", "cellular process", "localization",

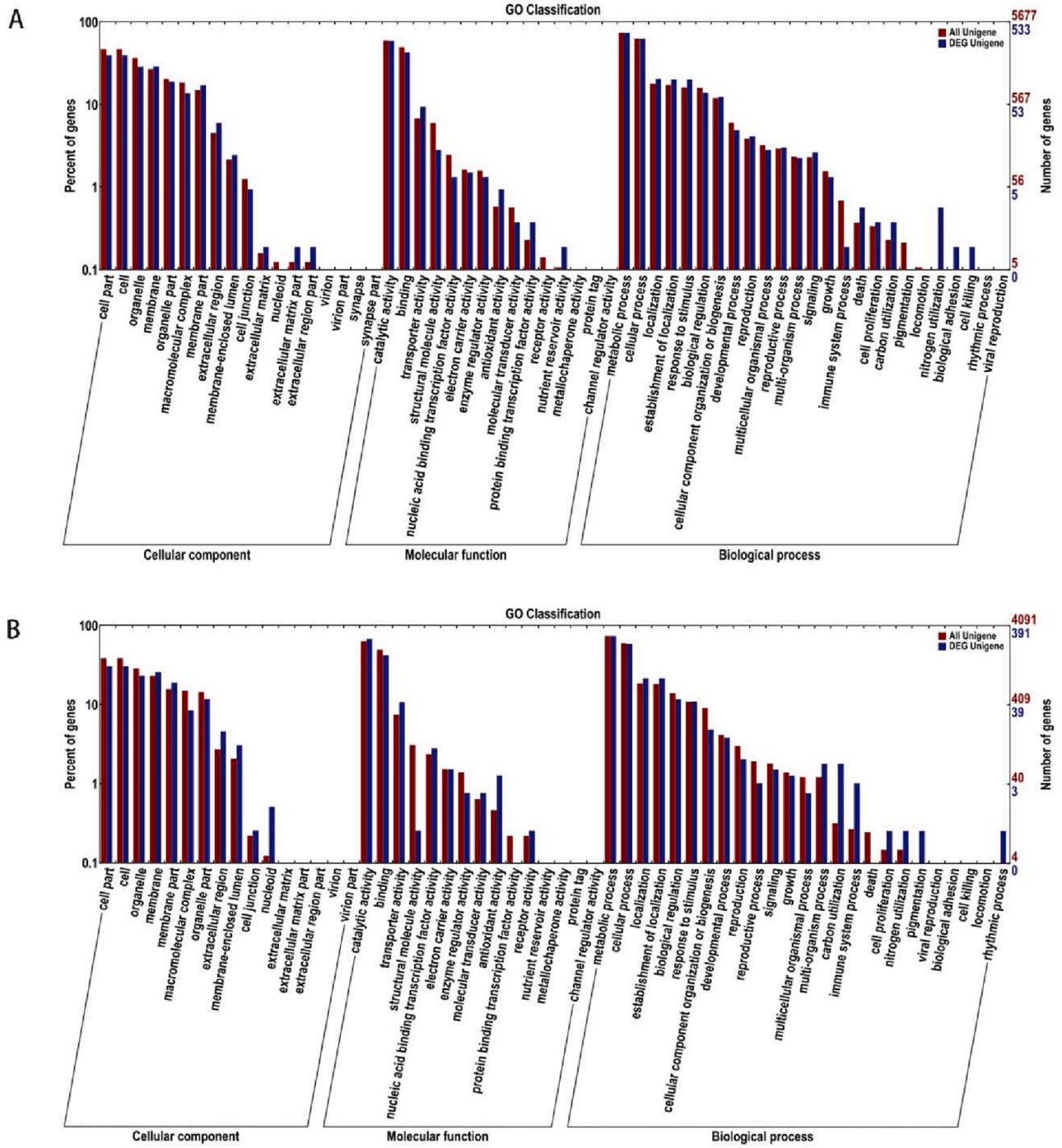

Fig. 4. (***A*** and ***B***) GO functional classification of DEGs in the *SP vs GP* and *GA vs GP* groups.

"establishment of localization", "biological regulation", "response to stimulus", "cellular component organization or biogenesis", "developmental process", and "reproduction" were the most mapped terms. The specific secondary metabolic pathways involved in the biosynthesis of the pigments needed to be assessed further via the KEGG metabolic pathway.

3.5. KEGG pathway enrichment of DEGs

Transcriptome data were explored furtherusing the KEGG pathway analysis. There were 65 and 70 pathways in the *SP vs GP* and *GA vs GP* groups, respectively (Fig. 5A & 5C; Table S3). The top four mapped pathways with the most number of DEGs in the *SP vs GP* group were as follows:"protein processing in the endoplasmic reticulum" (19 DEGs); "oxidative phosphorylation (11 DEGs)";"cysteine and methionine metabolism" (nine DEGs); and "ribosome" (nine DEGs). The top two mapped pathways with the most number of DEGs in the *GA vs GP* group were "oxidative phosphorylation" (nine DEGs) and "peroxisome" (eight DEGs). Based on the adjusted p-value (Q-value), KEGG pathways that were enriched in both groups were identified. The 20 most significantly enriched KEGG pathways are shown (Fig. 5C & 5D). "Fatty acid biosynthesis" was significantly enriched in the *SP vs GP* group. The transcription levels of five genes (c1647.graph_c0, c3643.graph_c0, c3666.graph_c0, c3907.graph_c0, and c6250.graph_c0) increased by

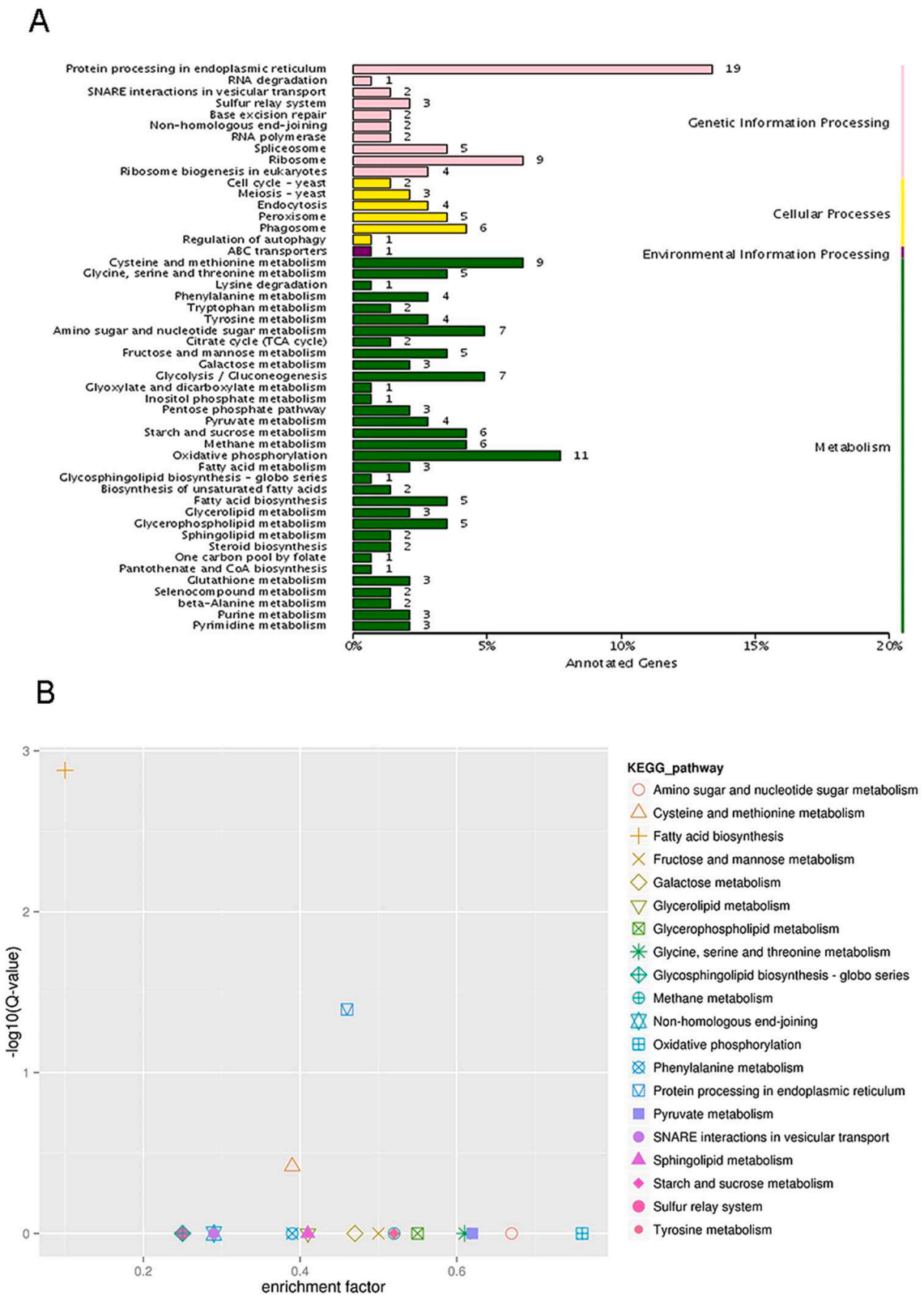

Fig. 5. (***A*** and ***B***) KEGG pathway enrichment of the *SP vs GP* group. (***C*** and ***D***) KEGG pathway enrichment of the *GA vs GP* group. The enrichment factor indicates the number of DEGs relative to the percentage of all annotated genes involved in the pathway.

1.50, 1.15, 1.40, 1.35, and 1.33 $\log_2$FC. They encoded fatty acid synthase alpha subunit FasA, acetyl-CoA carboxylase, fatty acid synthase beta subunit, putative agmatinase, and 3-oxoacyl-(acyl-carrier-protein) reductase. These findings suggest that the changes in fatty acid degradation were the main influences on pigment synthesis. "Glyoxylate and dicarboxylate metabolism" was significantly enriched in the *GA vs GP* group. The transcription levels of seven genes (c1219.graph_c0, c3184/4180.graph_c0, c5147.graph_c0, c5182.graph_c0, c5212.

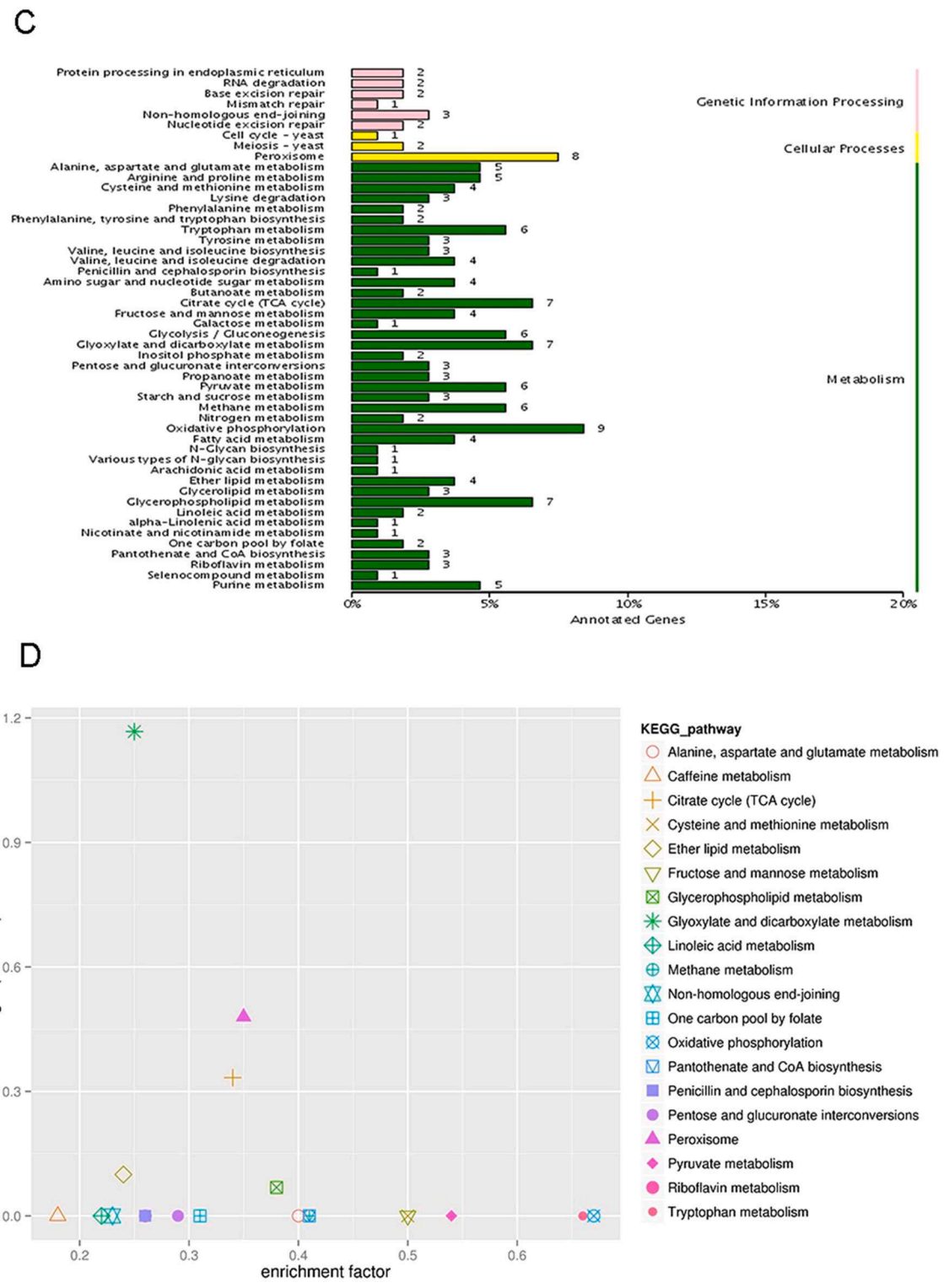

Fig. 5. (*continued*).

graph_c0, and c6568.graph_c0) decreased by 1.32, 1.79, 1.62, 2.58, 2.17, 1.71, and 4.84 $\log_2$FC.They encoded NAD-dependent formate dehydrogenase AciA/Fdh, citrate synthase Cit1, mitochondrial aconitate hydratase, isocitrate lyase AcuD, malate synthase AcuE, and a hypothetical protein.

Based on the adjusted *p*-value (Q-value), in the KEGG pathway, "fatty acid biosynthesis" was significantly enriched in the *SP vs GP* group. In the fatty acid biosynthesis pathway, fatty acid synthase alpha subunit FasA, acetyl-CoA carboxylase, fatty acid synthase beta subunit, putative agmatinase, and 3-oxoacyl-(acyl-carrier-protein) reductase were up-regulated, indicating that more fatty acids were synthesized in GP to produce caprylic acid, capric acid, lauric acid, myristic acid. Octanoic acid is an intermediate in the biosynthesis of MPs. Therefore, it might indicate that in addition to the obvious promotion effect of glycerol in the GP group, more acetyl-CoAs were generated in the above-mentioned metabolism to improve the yield of the pigments. Octanoic acid was also

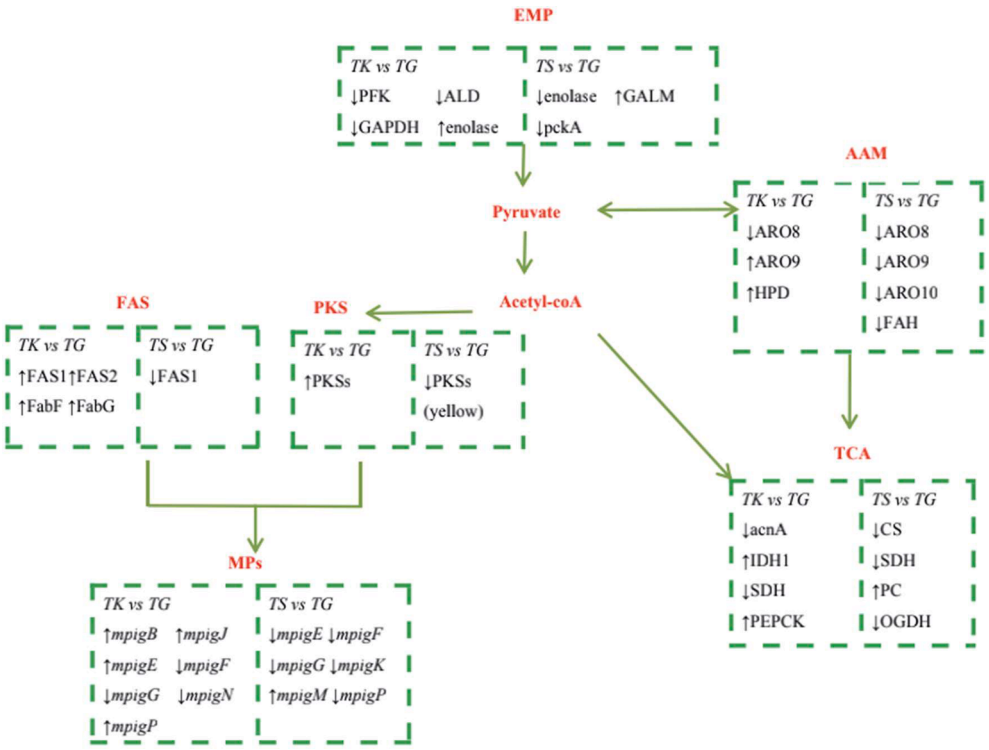

Fig. 6. Synthetic pathway of MPs (glycolysis-EMP, amino acid metabolism-AAM, fatty acid synthetic-FAS, polyketide synthase-PKS; ↑indicates up-regulated proteins and genes; ↓ indicates down-regulated proteins and genes).

up-regulated in fatty acid synthesis. Glyoxylate and dicarboxylate metabolism improved the ability of the organism to use acetyl-CoA, indicating that more acetyl-CoA was generated in GP.

3.6. Analysis of primary metabolism-related DEGs in MPs

Based on the results from the NR and Swiss-Prot databases (Table S4), in the *SP vs GP* group, the genes associated with the tricarboxylic acid (TCA) cycle included c4121.graph_c0, c6239.graph_c0, c7070.graph_c0, and c4969.graph_c0, which were annotated "aconitase", "isocitrate dehydrogenase", "succinate dehydrogenase", and "phosphoenolpyruvate carboxykinase", respectively. In the *GA vs GP* group, genes associated with the TCA cycle included c3184.graph_c0, c5666.graph_c0, c5863.graph_c0, and c5235.graph_c0, which were annotated "citrate synthase", "oxoglutarate dehydrogenase complex", "succinate dehydrogenase", and "pyruvate carboxylase", respectively. Acetyl-CoA was the important precursor of MPs; its metabolic network included the TCA cycle, glycolysis, glyoxylic acid cycle, amino acid metabolism, and pyruvate metabolism. Many enzymes and genes of the fatty acid synthetic pathway underwent significant changes in the *SP vs GP* and *GA vs GP* groups(Fig. 6).

Acetyl-CoA is the precursor of the primary metabolic pathway for MP synthesis and a critical metabolic intermediate in energy metabolism. The three macronutrients, sugar, fat, and protein, converge into a common metabolic pathway via acetyl-CoA in the TCA cycle and oxidative phosphorylation. Through this pathway, carbon dioxide and water are completely oxidized to release energy for ATP synthesis. Acetyl-CoA is also the precursor for the synthesis of cholesterol and its derivatives, and other physiologically active substances (Liang et al., 2018; Long et al., 2019; Zeng et al., 2021). The analysis of genes related to the primary metabolism of *Monascus* spp. showed that using glycerol as the carbon source and peptone as the nitrogen source could induce glycolysis, TCA cycle, pyruvate metabolism, glyoxylic acid cycle, amino acid metabolism (alanine, glutamic acid, tyrosine, and leucine), and fatty acid synthesis.

In the glycolytic pathway, galactosyl transferase is a galactose spinase that converts α-D-glucose to β-D-glucose. Enolase can convert 2-phosphoglycerate to phosphoenolpyruvate in the glycolytic pathway (Huang et al., 2016). Pyruvate is formed from enolpyruvateat the end of glycolysis. The genes encoding these enzymes were all significantly up-regulated in the *SP vs GP* group, revealing that glycolysis was significantly active in the intervention of glycerol compared with soluble starch, resulting in the production of more pyruvate and promoting the production of pigments.

3.7. Analysis of secondary metabolism-related DEGs in MPs

According to these results, the genes involved in the MP biosynthesis showed differential expressions in the comparisons between *SP vs GP* and *GA vs GP*. This indicates that pigment production is mediated by carbon and nitrogen. The expression of c1035.graph_c0 and c920.graph_c0a genes, transcriptional regulators of the pigment biosynthesis gene cluster, were up-regulated in the *SP vs GP* and *GA vs GP* groups (Fig. 6& Table S5). This indicates that the addition of glycerol and peptone induced the biosynthesis of pigments more compared with soluble starch. Transcription factors (TFs) can mediate the gene expression patterns to modulate the overall metabolism, including secondary metabolic pathways. Based on the NR database results, large number of genes related to the polyketide synthase pathway and pigment biosynthesis TFs was up-regulated when glycerol was adopted as the carbon source. Moreover, 24 and 32 differentially expressed TFs were activated by carbon and nitrogen, respectively. The gene c1122.graph_c0 encoded a TF that played a regulatory role in nitrogen metabolism. Changes occurred in the expressions of TFs following the KEGG pathways, revealing that carbon/nitrogen affected TF expression (Table S6).

4. Conclusion

In this study, a comparative transcriptional approach was adopted to

explore the regulatory effects of carbon and nitrogen on the biosynthesis of MPs. We also investigated the impact of carbon/nitrogen on the secondary metabolism and gene transcription of *M. kaoliang* in liquid fermentation, providing comprehensive knowledge of the links between primary and secondary metabolisms. The results of the sequencing assay indicate that GP was capable of significant gene enrichment in the classification of carbohydrate catabolism, energy synthesis and metabolism, amino acid metabolism, lipid metabolism, and secondary metabolism. Transcriptome analysis highlighted the differences in the expression of pigment biosynthesis-related genes and provided valuable insights into genes related regulatory mechanisms involved in other energetic metabolisms and biological processes.

Funding

The project was supported by Double First-Class Construction Plan (KSYLX013) of Fujian Agriculture and Forestry University and the Open Project Program of the Key Laboratory of Brewing Molecular Engineering of China Light Industry (BME-202004).

Declaration of Competing Interest

The authors declare that they have no known competing financial interests or personal relationships that could have appeared to influence the work reported in this paper.

Appendix A. Supplementary data

Supplementary data to this article can be found online at https://doi.org/10.1016/j.fochx.2022.100250.

References

Agboyibor, C., Kong, W.-B., Chen, D., Zhang, A.-M., & Niu, S.-Q. (2018). *Monascus* pigments production, composition, bioactivity and its application: A review. *Biocatalysis and Agricultural Biotechnology, 16*, 433–447.

Aniya, Y., Ohtani, I. I., Higa, T., Miyagi, C., Gibo, H., Shimabukuro, M., et al. (2000). Dimerumic acid as an antioxidant of the mold *Monascus anka*. *Free Radical Biology & Medicine, 28*(6), 999–1004.

Chen, D., Chen, M. H., Wu, S. F., Li, Z. J., Yang, H., & Wang, C. L. (2017). Themolecular mechanisms of *Monascus purpureus* M9responses to blue light based on the transcriptome analysis. *Scientific Reports, 7*(1), 1–10.

Chen, W., Chen, R., Liu, Q., He, Y.i., He, K., Ding, X., et al. (2017). Orange, red, yellow: Biosynthesis of azaphilone pigments in *Monascus fungi*. *Chemical Science, 8*(7), 4917–4925.

Chen, W., He, Y.i., Zhou, Y., Shao, Y., Feng, Y., Li, M.u., et al. (2015). Edible filamentous fungi from the species *Monascus*: Early traditional fermentations, modern molecular biology, and future genomics. *Comprehensive Reviews in Food Science & Food Safety, 14*(5), 555–567.

Diana, M., Quílez, J., & Rafecas, M. (2014). Gamma-aminobutyric acid as a bioactive compound in foods: A review. *Journal of Functional Foods, 10*, 407–420.

Embaby, A. M., Hussein, M. N., Hussein, A., & Papp, T. (2018). *Monascus* orange and red pigments production by *Monascus purpureus* ATCC 16436 through co-solid state fermentation of corn cob and glycerol: An eco-friendly environmental low cost approach. *Plos One, 13*(12), e0207755.

Klinsupa, W., Phansiri, S., Thongpradis, P., Yongsmith, B., & Pothiratana, C. (2016). Enhancement of yellow pigment production by intraspecific protoplast fusion of *Monascus* spp. yellow mutant (ade-) and white mutant (prototroph). *Journal of Biotechnology, 217*, 62–71.

Hajjaj, H., Goma, G., & François, J. M. (2015). Effect of the cultivation mode on red pigments production from *Monascus ruber*. *International Journal of Food Science & Technology, 50*(8), 1731–1736.

Hong, J.-L., Wu, L.i., Lu, J.-Q., Zhou, W.-B., Cao, Y.-J., Lv, W.-L., et al. (2020). Comparative transcriptomic analysis reveals the regulatory effects of inorganic nitrogen on the biosynthesis of *Monascus* pigments and citrinin. *RSC. Advances, 10*(9), 5268–5282.

Huang, Z.-R., Zhou, W.-B., Yang, X.-L., Tong, A.-J., Hong, J.-L., Guo, W.-L., et al. (2018). The regulation mechanisms of soluble starch and glycerol for production of azaphilone pigments in *Monascus purpureus*FAFU618 as revealed by comparative proteomic and transcriptional analyses. *Food Research International, 106*, 626–635.

Huang, Z., Zhang, S., Xu, Y., Li, L., & Li, Y. (2016). Metabolic effects of the *pksct* gene on *Monascus aurantiacus* Li As3.4384 using gas chromatography–time-of-flight mass spectrometry-based metabolomics. *Journal of Agricultural and Food Chemistry, 64*(7), 1565–1574.

Li, L., Shao, Y. C., Li, Q., Yang, S., & Chen, F. S. (2010). Identification of Mga1, a G-protein α-subunit gene involved in regulating citrinin and pigment production in *Monascus ruber* M7. *FEMS Microbiology Letters., 308*(2), 108–114.

Li, Z. Q., & Guo, F. (2003). *Morphology and taxonomy of Monascus* (1th ed.). Longman (Chapter 4).

Li, Z. Q., Yang, X. T., & Guo, F. (2009). *An overview of red yeast rice and red yeast rice* (1st ed.). Longman (Chapter 6).

Liang, B., Du, X. J., Li, P., Sun, C. C., & Wang, S. (2018). Investigation of citrinin and pigment biosynthesis mechanisms in *Monascus purpureus* by transcriptomic analysis. *Frontiers in Microbiology, 9*, 1374.

Lin, T. F., & Demain, A. L. (1995). Negative effect of ammonium nitrate as nitrogen source on the production of water-soluble red pigments by *Monascus* spp. *Applied Microbiology and Biotechnology, 43*(4), 701–705.

Liu, J., Wu, J., Cai, X., Zhang, S., & Lin, Q. (2020). Regulation of secondary metabolite biosynthesis in *Monascus purpureus* via cofactor metabolic engineering strategies. *Food Microbiology, 95*(13), Article 103689.

Long, C., Zeng, X.u., Xie, J., Liang, Y., Tao, J., Tao, Q., et al. (2019). High-level production of *Monascus* pigments in *Monascus ruber* CICC41233 through atp-citrate lyase overexpression. *Biochemical Engineering Journal, 146*, 160–169.

Lv, X. C., Wu, X., Han, M., Zhang, W., Rao, P., & Ni, L. (2012). Identification and characterization of *Monascus* spp. from Fujian hongqu. *Journal of Chinese Institute of Food Science and Technology, 12*(2), 88–97.

Mapari, S. A. S., Thrane, U., & Meyer, A. S. (2010). Fungal polyketide azaphilone pigments as future natural food colorants? *Trends in Biotechnology, 28*(6), 300–307.

Nam, K., Choe, D., & Shin, C. S. (2014). Antiobesity effect of a jelly food containing the L-tryptophan derivative of *Monascus* pigment in mice. *Journal of Functional Foods, 9*(1), 306–314.

Patrovsky, M., Sinovska, K., Branska, B., & Patakova, P. (2019). Effect of initial pH, different nitrogen sources, and cultivation time on the production of yellow or orange *Monascus purpureus* pigments and the mycotoxin citrinin. *Food Science & Nutrition, 7*(11), 3494–3500.

Park, K. H., Liu, Z., Park, C.-S., & Ni, L.i. (2016). Microbiota associated with the starter cultures and brewing process of traditional hong qu glutinous rice wine. *Food Science and Biotechnology, 25*(3), 649–658.

Said, F. M., Brooks, J., & Chisti, Y. (2014). Optimal C: N ratio for the production of red pigments by*Monascusruber*. *World Journal of Microbiology and Biotechnology, 30*(9), 2471–2479.

Shi, J., Zhao, W., Lu, J., Wang, W., & Feng, Y. (2020). Insight into *Monascus* pigments production promoted by glycerol based on physiological and transcriptome analyses. *Process Biochemistry, 102*(1), 141–149.

Shi, K., Song, D.a., Chen, G., Pistolozzi, M., Wu, Z., & Quan, L. (2015). Controlling composition and color characteristics of *Monascus* pigments by pH and nitrogen sources in submerged fermentation. *Journal of Bioscience and Bioengineering, 120*(2), 145–154.

Yang, S., Zhou, H., Dai, W., Xiong, J., & Chen, F. (2021). Effect of static magnetic field on *Monascus ruber* M7 based on transcriptome analysis. *Journal of Fungi, 7*(4), 256. https://doi.org/10.3390/jof7040256

Yasukawa, K., Takahashi, M., Yamanouchi, S., & Takido, M. (1996). Inhibitory effect of oral administration of *Monascus* pigments on tumor promotion in two-stage carcinogenesis in mouse skin. *Oncology, 53*(3), 247–249.

Zeng, C., Yoshizaki, Y., Yin, X., Wang, Z., Okutsu, K., Futagami, T., et al. (2021). Additional moisture during koji preparation contributes to the pigment production of red koji (*Monascus*-fermented rice) by influencing gene expression. *Journal of Food Science, 86*(3), 969–976.

Zhang, R., Yu, J., Guo, X., Li, W., Xing, Y., & Wang, Y. (2021). *Monascus* pigment-ediated green synthesis of silver nanoparticles: Catalytic, antioxidant, and antibacterial activity. *Applied Organometallic Chemistry, 35*(3), Article e6120.

Zhao, W., Yao, Y., Wang, S., Shi, J., Shu, S., & Feng, Y. (2019). Exploration on carbon source selectivity of glycerol affecting pigments production by *Monascus* spp. *Journal of Microbiology, 39*(5), 28–34.

Zhou, B., Ma, Y. F., Tian, Y., Li, J. B., & Zhong, H. Y. (2020). Quantitative proteomics analysis by sequential window acquisition of all theoretical mass spectra–mass spectrometry reveals inhibition mechanism of pigments and citrinin production of *Monascus* response to high ammonium chloride concentration. *Journal of Agricultural and Food Chemistry, 68*(3), 808–817.